# Object Discrimination Using Optimized Multi-frequency Auditory Cross-Modal Haptic Feedback

Alison Gibson and Panagiotis Artemiadis
Mechanical and Aerospace Engineering
School for Engineering of Matter, Transport and Energy
Arizona State University
Tempe, AZ 85287 USA
Email: {aegibson, panagiotis.artemiadis}@asu.edu

***Abstract*—As the field of brain-machine interfaces and neuro-prosthetics continues to grow, there is a high need for sensor and actuation mechanisms that can provide haptic feedback to the user. Current technologies employ expensive, invasive and often inefficient force feedback methods, resulting in an unrealistic solution for individuals who rely on these devices. This paper responds through the development, integration and analysis of a novel feedback architecture where haptic information during the neural control of a prosthetic hand is perceived through multi-frequency auditory signals. Through representing force magnitude with volume and force location with frequency, the feedback architecture can translate the haptic experiences of a robotic end effector into the alternative sensory modality of sound. Previous research with the proposed cross-modal feedback method confirmed its learnability, so the current work aimed to investigate which frequency map (i.e. frequency-specific locations on the hand) is optimal in helping users distinguish between hand-held objects and tasks associated with them. After short use with the cross-modal feedback during the electromyographic (EMG) control of a prosthetic hand, testing results show that users are able to use audial feedback alone to discriminate between everyday objects. While users showed adaptation to three different frequency maps, the simplest map containing only two frequencies was found to be the most useful in discriminating between objects. This outcome provides support for the feasibility and practicality of the cross-modal feedback method during the neural control of prosthetics.**

## I. Introduction

Force feedback during the operation of robotic end effectors has become a priority due to the potential of its control benefits and the fact that it has been so widely requested by those using prosthetic devices; according to results from a questionnaire administered through Orthopedic University Hospital Heidelberg, the most desired additional function for prosthetic devices is force feedback [1]. Current systems in brain-machine interface technology (e.g. neuro-prosthetics, exoskeletons, robotic teleoperation) use mostly visual feedback during operation, which does not relay information about contact forces involved during use of the end-effector. While visual information certainly aids users during control tasks and interactions, this information can be irrelevant during force-sensitive motions (e.g. handshake) or situations where visual feedback may not be available or sufficient. Not only is force regulation important in these contexts, but information about contact force location can also be beneficial in object discrimination, tactile exploration and overall dexterous control.

Haptic feedback techniques currently in use are often invasive, costly and thus come with severe limitations. Intra-cortical microstimulation of brain sensory areas [2], targeted reinnervation of residual sensory nerves [3]–[5] and electrical stimulation via brain implants [6] all involve expensive and potentially harmful surgeries and modifications. Other methods in use that are less invasive include the use of haptic tactors [6] or vibrotactile technologies [7], [8], which can be useful in exoskeleton operation or some forms of robotic teleoperation, yet are not viable solutions for persons with a missing hand or limb. In response to these limitations, this paper proposes an alternative, sensory-substitutive feedback technique where contact forces are perceived through multi-frequency auditory signals. Through representing force magnitude with volume and force location with frequency, the feedback architecture can translate the haptic experiences of a robotic end effector into the alternative sensory modality of sound. User adaptation to this kind of sensory substitution is supported through well-studied neural mechanisms that constitute neural plasticity; within this paradigm, a more specific cross-modal plasticity is believed to enable the integration of separate sensory modalities over time [9], [10]. In addition, a body of neuroscience literature suggests that a form of supra-additive integration of sound and touch already occurs in associated regions of the brain [11]–[14]. These implications provide support for user adaptation to the proposed feedback method, suggesting it can be a realistic and user-friendly technology.

A prototype of the cross-modal feedback architecture was developed and used in a series of closed-loop control experiments, with results providing immense support for its learnability [15]. In order to examine whether or not certain frequency maps can provide more detailed information about objects and end effector configurations, the current experiment had users grasp everyday objects requiring disparate hand configurations while utilizing one of three different frequency maps. After this training phase, users were tested in using audial feedback alone to discriminate between objects used in the learned tasks.

978-1-4244-7929-0/14/$26.00 ©2014 IEEE

## II. METHODS

### A. Feedback Architecture

An i-Limb Ultra prosthetic robotic hand (Touchbionics Inc) is equipped with a glove containing twenty 0.4" diameter Force Sensing Resistor sensors (Flexiforce FSR), which are split up into different regions that depend on frequency assignment, as shown in Fig. 1. There are three frequency regions for the original and radial maps, while there are only two regions for the biregion map. The original map was successfully used in previous experiments, while the radial and biregion maps were designed specifically for this analysis. The radial map was chosen in order to examine whether or not forces applied on outer parts of the hand had a significant effect on the sound signals associated with various objects. The biregion map was designed to be the simplest layout in order to observe whether such simplicity assists in learning this technology for the first time.

Each map has its own circuit, where the sensors belonging to a single frequency region are all connected in parallel to each other and then finally in series with a terminal resistor. When using one of the circuit prototypes, a 5V voltage is connected in parallel to the total system and the total voltage across the terminal resistor of each region is connected to an Analog Input port of a microcontroller (Arduino MEGA 2560 R3). When forces are not being exerted on an FSR, the force sensor acts as an infinite resistance and therefore the terminal resistor voltage drop is zero (open circuit). Conversely, during any applied force, the resistance of the force sensor linearly decreases with respect to the force magnitude, making the total analog voltage across a force sensor decrease as the exerted force on it increases. Consequently, the voltage drops across the terminal resistors increase, and therefore each region has an associated voltage input representing the sum of forces experienced in that region. $V_R^{(i)}$ represents the voltage across a terminal resistor within a region $i$ ($i$=1,2,3 for the original and radial map while $i$=1,2 for the bi-region map); therefore, $\sum_{n_i} F_{n_i}$ represents the sum of the forces exerted on the $n_i$ sensors within that region, so the total voltage measured by the micro-controller for each region is given by:

$$V_R^{(i)} = K \sum_{n_i} F_{n_i} \tag{1}$$

where $K$ is the gain of the sensors converting the sensed force to voltage.

Hence, the generated sound signal $X(t)$ represents all forces across all regions, where $t$ represents time and $X(t)$ is given by:

$$X(t) = \sum_{i=1}^{n_R} \frac{1}{n_R} \frac{V_R^{(i)}}{V_R^{max}} \sin(2\pi f_i t) \tag{2}$$

where the division by the amount of regions in the map ($n_R$) ensures that each region is weighted equally, $V_R^{max}$ is the maximum voltage that can be measured from each analog input (i.e. 5V), and $f_i$ is the frequency assigned to that region. The frequency map regions currently have possible assignments of 200 Hz, 300 Hz and 400 Hz. The signal $X(t)$ will always be within the range [-1,1]V and its frequency components will be a function of the total forces exerted within each region. For example, if most of the forces are applied to the sensors within a region with frequency assignment of 200 Hz, then a 200 Hz frequency will dominate in the resultant sound signal. This resultant sound signal is output through a separate analog output of the microcontroller and received by Audio-Technica ATH-ANC9 headphones. The volume and frequency components of this sound signal are updated every $64ms$ to constitute a real-time experience with minimal delay.

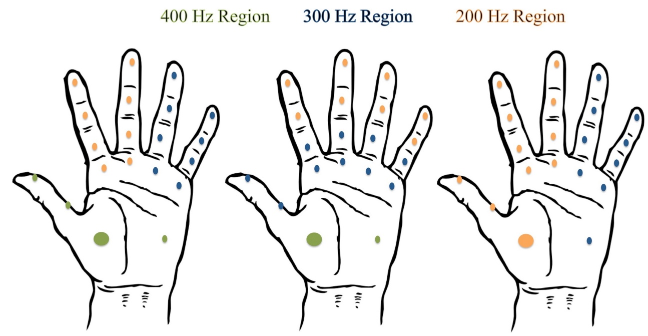


Fig. 1. From left to right: Original Map, Radial Map and Biregion Map.

### B. EMG Control Algorithm

An EMG system with wireless electrodes (Trigno Wireless, Delsys Inc) was used for acquiring EMG signals from the forearm of human subjects in order to control the opening and closing of the fingers of the robotic prosthesis. An extensor muscle (Extensor Carpi Ulnaris) on the forearm was chosen to be responsible for actuating the opening of the robotic hand at velocities directly correlated to the muscle co-contraction level; for closing the hand, a flexor muscle (Flexor Carpi Radialis) was chosen and utilized in an equivalent manner. Prior to using the system, each user is told to contract the extensor and flexor muscles to their maximum potential during wrist extension and wrist flexion so that each muscle's maximum voltage level, $V_{max}$, can be recorded. Each user is then instructed to relax the forearm so that each muscle's minimum voltage level, $V_{min}$, can also be recorded. After these parameters are collected, real-time use of the system can begin.

The raw EMG signals undergo a pre-processing stage that is commonly used in the field of electromyography to compute the linear envelope of the signal [16]. The linear envelope performs full-wave rectification of the raw signals prior to passing them through a low pass filter (2nd order Butterworth, cut-off frequency of 8 Hz). After this step, EMG signals for each muscle are normalized with respect to the muscle's $V_{max}$ [17]. This process essentially simplifies and reduces noise in the signals before quickly calibrating the system to the user's muscular characteristics.

The five-fingered robotic prosthesis controller allows for the control of each finger's velocity within the range of 25 to 65 deg/s. Each finger is underactuated, therefore only one motor controls the flexion or extension of each of three finger joints (proximal, middle, distal). There are 14 different values for velocity that can be commanded to each finger, namely $\pm 1 \ldots \pm 7$, which correspond to 7 different values equally spaced in the range of 25 to 65 deg/s, for positive (opening) and negative (closing) velocities. When a velocity value is commanded to a finger, the finger will start moving with that

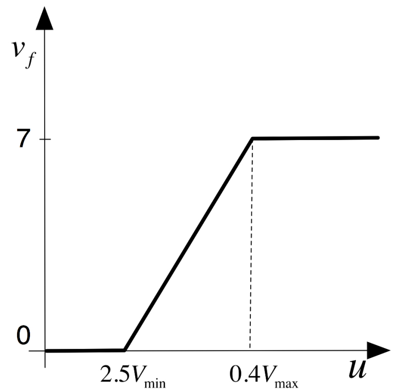


Fig. 2. Commanded absolute finger velocity as a function of normalized EMG signal.

velocity until it encounters a pre-defined maximum opposing force, which is a function of that velocity. Therefore, in the case that a finger physically interacts with the environment, control of velocity results in indirect control of force exerted from the finger on the environment. Consequently, the control of velocity for each finger can be associated with the control of each finger's force when the finger is in contact with an object, i.e. grasping. The maximum power grip force of the prosthesis is 100N.

The processed EMG signals are used in real-time to directly control the velocity at which the robotic hand opens and closes, where increased muscle contraction results in an increase in velocity in the direction associated with that muscle. While the extensor and flexor muscles both play a role in each of these opposing motions, prior research [18] and electromyography convention [17] suggest that extensor muscle activation is much higher for wrist extension while flexor muscle activation is much higher for wrist flexion. These relationships provide a basis for the EMG-control algorithm, which quantitatively compares the averages of the normalized signals in $100ms$ windows. If the maximum value of the processed EMG signal $u$ within the window is greater than 2.5 times the relaxation voltage $V_{min}$ of the specific muscle, the hand is commanded to either close or open all fingers simultaneously, depending on the muscle activated. The function that determines actuation velocity from normalized EMG signals employs the user-specific $V_{max}$ and $V_{min}$ collected prior. Once the muscle reaches a level greater than 40% of the user's $V_{max}$, the velocity is at maximum. The function that gives the absolute finger velocity $v_f$ based on the processed EMG signal $u$ is given by:

$$v_f = \begin{cases} 0 & , u < 2.5V_{\min} \\ \lceil \frac{7}{0.4 - V_{\min}} u + 7 - \frac{2.8}{0.4 - V_{\min}} \rceil & , 2.5V_{\min} \leq u < 0.4V_{\max} \\ 7 & , u \geq 0.4V_{\max} \end{cases} \tag{3}$$

where $\lceil x \rceil$ represents the ceiling function, i.e. rounding of the number $x$ to the nearest integer towards plus infinity. Fig. 2 shows the relationship between EMG magnitude and actuation velocity.

### C. Experiment Protocol

The experiment consisted of two phases: 1) Training with the feedback method for three tasks requiring different hand configurations, and 2) A blind-folded testing where users could only use audial feedback to discriminate which object was in the robotic hand. Twelve healthy subjects (20-30 years old) all gave informed consent according to procedures approved by the ASU IRB (Protocol: #1201007252). Three frequency maps were used (shown in Fig. 1), where 4 different users were assigned to a map, resulting in 12 total users. Subjects 1-4 used the "Original" frequency Map, subjects 5-8 used the "Radial" frequency map and subjects 9-12 used the "Biregion" frequency map. In addition, the time it took for each subject to firmly grasp the object with the robotic hand was recorded for all trials.

*1) Training Phase:* Users were instructed to grasp three different objects with the i-Limb Ultra robotic hand, all of which required different hand configurations. The objects included a marker (placed against the palm of the hand with the thumb apposed), a foam ball (placed against the palm with the thumb opposed) and a key (placed between the index and thumb fingers with the thumb opposed). Hence, the only adjustments made to the robotic hand between trials was thumb opposition and apposition, a function commonly found in hand prostheses. During each of 24 trials (8 per object), the object was placed into the robotic hand by the experimenter and the user utilized EMG-control of the opening/closing motion while listening to the audial feedback on Audio-Technica ATH-ANC9 headphones. The experimental setup is shown in Fig. 3.

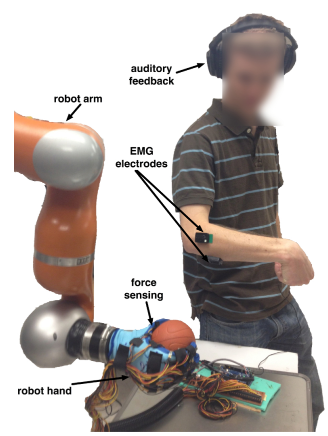


Fig. 3. Experimental setup.

*2) Blind-folded Testing Phase:* Users employed the same grasping control as before, except were blind-folded and told to use audial feedback alone to guess which objects were placed in the robotic hand by the experimenter. For each trial, users earned a qualitative accuracy score where a correct guess received a $score = 1$ and an incorrect guess received a $score = 0$. The user's final accuracy score was then found by adding up the trial scores and dividing by the total trials to get a percentage reflective of test performance.

## III. RESULTS

The trial completion times (time for the user to achieve firm grasp of the object) during the training phase were normalized for each trial with respect to the maximum trial time for each subject. Results are shown in Fig. 4. The decrease in both completion time and variance for trials involving the ball and key suggest a form of user learning and adaptation to the feedback. Conversely, completion times for the marker trials don't show a reduction in trial time or variance throughout

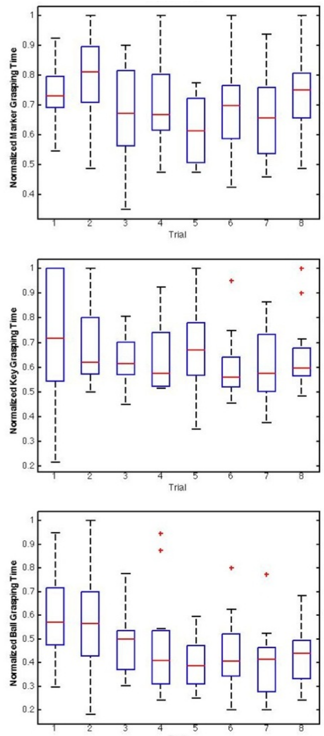


Fig. 4. From top to bottom: Marker Trials, Ball Trials and Key Trials, for all (12) subjects.

TABLE I. USER TEST SCORES FOR EACH FREQUENCY MAP

| **User** | 1 | 2 | 3 | 4 | **Average** |
|---|---|---|---|---|---|
| **Map** | Original | Original | Original | Original | Original |
| **Score** | 67% | 100% | 83% | 83% | 83% |
| **User** | 5 | 6 | 7 | 8 | **Average** |
| **Map** | Radial | Radial | Radial | Radial | Radial |
| **Score** | 100% | 83% | 83% | 83% | 87% |
| **User** | 9 | 10 | 11 | 12 | **Average** |
| **Map** | Biregion | Biregion | Biregion | Biregion | Biregion |
| **Score** | 100% | 100% | 100% | 100% | 100% |

training. The average trial time and standard deviation across all users and trials was $2.7s$ and $0.7s$, respectively.

Most importantly, results demonstrate that users were able to associate specific sound signals to objects. According to the blindfold test scores for all users reflected in Table I, all three frequency maps enabled users to successfully discriminate between objects. The biregion map shows to be the most useful in helping users differentiate between objects and tasks, which could possibly be due to the map's simplicity in only having two frequencies; since the feedback method is a newly learned sensory substitutive experience for the users, it's evident that the simplest form of the technology would be easiest to learn in the short time given.

## IV. Conclusion

This paper investigated the effect of different frequency maps on user capabilities to discriminate between hand-held objects while using an alternative haptic feedback method. After a simple training phase using common, everyday objects in grasping tasks with a robotic hand, users were able to use the cross-modal audial feedback alone to determine which object the robotic hand was holding. Results further support the learnability and practicality of the proposed sensory substitutive feedback method, a non-invasive and efficient technique for perceiving force feedback in anthropomorphic robotic operation.

## References


[1] C. Pylatiuk, S. Schulz, and L. Döderlein, "Results of an internet survey of myoelectric prosthetic hand users," *Prosthetics and orthotics international*, vol. 31, no. 4, pp. 362–370, 2007.

[2] L. E. Medina, M. A. Lebedev, J. E. O'Doherty, and M. A. Nicolelis, "Stochastic facilitation of artificial tactile sensation in primates," *The Journal of Neuroscience*, vol. 32, no. 41, pp. 14 271–14 275, 2012.

[3] T. A. Kuiken, P. D. Marasco, B. A. Lock, R. N. Harden, and J. P. Dewald, "Redirection of cutaneous sensation from the hand to the chest skin of human amputees with targeted reinnervation," *Proceedings of the National Academy of Sciences*, vol. 104, no. 50, pp. 20 061–20 066, 2007.

[4] J. W. Sensinger, T. Kuiken, T. R. Farrell, and R. F. Weir, "Phantom limb sensory feedback through nerve transfer surgery." Myoelectric Symposium, 2005.

[5] P. D. Marasco, K. Kim, J. E. Colgate, M. A. Peshkin, and T. A. Kuiken, "Robotic touch shifts perception of embodiment to a prosthesis in targeted reinnervation amputees," *Brain*, vol. 134, no. 3, pp. 747–758, 2011.

[6] C. S. Armiger, K. D. Katyal, A. Makhlin, M. L. Natter, J. E. Colgate, S. J. Bensmaia, R. J. Vogelstein, M. S. Johannes, and F. V. Tenore, "Enabling closed-loop control of the modular prosthetic limb through haptic feedback," vol. 31, no. 4, pp. 345–353.

[7] C. Cipriani, M. D'Alonzo, and M. C. Carrozza, "A miniature vibrotactile sensory substitution device for multifingered hand prosthetics," *Biomedical Engineering, IEEE Transactions on*, vol. 59, no. 2, pp. 400–408, 2012.

[8] E. Rombokas, C. E. Stepp, C. Chang, M. Malhotra, and Y. Matsuoka, "Vibrotactile sensory substitution for electromyographic control of object manipulation," 2013.

[9] J. Wang and et al., "Basic experimental research on electrotactile physiology for deaf auditory substitution," vol. 35, no. 1, pp. 1–5.

[10] P. Bach-y Rita, *Brain mechanisms in sensory substitution*. Academic Press New York, 1972.

[11] M. S. Beauchamp, "See me, hear me, touch me: multisensory integration in lateral occipital-temporal cortex," *Current opinion in neurobiology*, vol. 15, no. 2, pp. 145–153, 2005.

[12] G. Caetano and V. Jousmäki, "Evidence of vibrotactile input to human auditory cortex," *Neuroimage*, vol. 29, no. 1, pp. 15–28, 2006.

[13] C. Kayser, C. I. Petkov, M. Augath, and N. K. Logothetis, "Integration of touch and sound in auditory cortex," *Neuron*, vol. 48, no. 2, pp. 373–384, 2005.

[14] M. Schürmann, G. Caetano, Y. Hlushchuk, V. Jousmäki, and R. Hari, "Touch activates human auditory cortex," *Neuroimage*, vol. 30, no. 4, pp. 1325–1331, 2006.

[15] A. E. Gibson and P. Artemiadis, "Closed-loop neural control of a hand prosthesis using cross-modal haptic feedback," in *Proceedings of the 2014 Intelligent Robots and Systems Conference (in review)*, 2014.

[16] F. E. Zajac, "Muscle and tendon: properties, models, scaling, and application to biomechanics and motor control." *Critical reviews in biomedical engineering*, vol. 17, no. 4, pp. 359–411, 1988.

[17] E. Criswell, *Cram's introduction to surface electromyography*. Jones & Bartlett Publishers, 2010.

[18] A. E. Gibson, M. R. Ison, and P. Artemiadis, "User-independent hand motion classification with electromyography," in *Proceedings of the 2013 Dynamic Systems and Controls Conference*, 2013.